APPLIED GEOPHYSICS, Vol.13, No.1 (March 2016), P. 166-178, 8 Figures.
DOI:10.1007/s11770-016-0532-6

Anisotropic rock physics models for interpreting pore structures in carbonate reservoirs*

Li Sheng-Jie♦[1,2], Shao Yu[3], and Chen Xu-Qiang[1,2]

Abstract: We developed an anisotropic effective theoretical model for modeling the elastic behavior of anisotropic carbonate reservoirs by combining the anisotropic self-consistent approximation and differential effective medium models. By analyzing the measured data from carbonate samples in the TL area, a carbonate pore-structure model for estimating the elastic parameters of carbonate rocks is proposed, which is a prerequisite in the analysis of carbonate reservoirs. A workflow for determining elastic properties of carbonate reservoirs is established in terms of the anisotropic effective theoretical model and the pore-structure model. We performed numerical experiments and compared the theoretical prediction and measured data. The result of the comparison suggests that the proposed anisotropic effective theoretical model can account for the relation between velocity and porosity in carbonate reservoirs. The model forms the basis for developing new tools for predicting and evaluating the properties of carbonate reservoirs.
Keywords: anisotropy, rock physics, pore structure, modulus, carbonates

Introduction

Rock physics models play a very important role in seismic data inversion and interpretation by relating rock properties (e.g., porosity, permeability, shale content, water saturation, pore structures etc.) and seismic attributes (e.g., seismic reflectivity, impedances, velocity, attenuation, etc). With the development of quantitative seismic interpretations, rock physics modeling is indispensable for studying complex reservoirs (Carcione and Avseth,, 2015).

Many of the rock physics models used in seismic exploration are empirical (e.g., Castagna et al., 1985; Krief et al., 1990) and typically assume a linear relation between velocity and porosity. Such empirical models perform well in some but not all areas. Generally, they are suitable for analyzing similar rocks within the area where the empirical models were formulated. Consequently, to use this type of empirical models to predict the properties of different reservoir, there is significant prediction error. Furthermore, the discrepancy between model predictions and measured data is large when insufficient data are used to calibrate the models. Hence such empirical models cannot be used to interpret the complex pore structure of heterogeneous carbonate

Manuscript received by the Editor January 1, 2015; revised manuscript received January 1, 2016.
*This work was supported by the National Natural Science Foundation of China (No. 41274136).
1. State Key Laboratory of Petroleum Resource and Prospecting, China University of Petroleum (Beijing), Beijing 102249, China.
2. CNPC Key Lab of China University of Petroleum (Beijing), Beijing 102249, China.
3. Research Institute of Exploration and Development, Xinjiang Oilfield, PetroChina, Karamay, Xinjiang 83400, China.
♦Corresponding author: Li Sheng-Jie (Email: Richard@cup.edu.cn)

reservoirs. Consequently, rock physics models that can account for the elastic properties of complex carbonate reservoirs are needed.

The carbonate matrix typically consists of several components with variable grain size, connected or unconnected pores of variable shape, and different pore-filling materials (e.g., fluid, debris). All these make carbonates a strongly heterogeneous composite medium. It is well known that the elastic properties of carbonate reservoirs are anisotropic and the degree of elastic anisotropy depends on many factors, that is, the distribution of mineral grains, the preferred orientation of pore structure and connectivity, the presence of cracks or fault zones, and the local principal stress. Among these factors, the preferred orientation of fractures and cavities in the carbonate reservoirs is one of the main factors causing seismic anisotropy. Landro (2015) derived an analytical aspect ratio relations between 2D eliipses and 3D ellisoids; Regnet et al (2015) found that micrite particle size and morphology affected elastic properties of carbonate rocks; Huang et al (2015) discussed the method of fluid substitution in complex pore structure and the effect of fluid substitution on seismic responses; Yu et al (2014) studied the relation between seismic responses and fluid properties in carbonate reservoirs; Li and Chen (2013) described a method of modelling elastic properties in carbonate rocks at seismic frequency.

Many theoretical rock physics models are used to characterize heterogeneous porous media. Several of them consider the heterogeneous medium as an equivalent homogeneous elastic material. This type of models is known as the effective medium model. Most homogeneous effective medium models are based on isotropic models to treat the solid matrix and pore fluids, ignoring the coupling between the rock skeleton and pore fluids. Consequently, such models can only be used to model sparsely distributed porous media, which limits their application. Under long wavelength conditions, the differential effective medium (DEM) and self-consistent approximation (SCA) models can be used to determine the elastic properties of isotropic, saturated porous media iteratively. Nonetheless, the DEM and SCA models only give us the elastic parameters of media with isolated inclusions.

Existing effective medium models of heterogeneous media cannot be used to directly estimate the elastic parameters of carbonate reservoirs. Xu and White (1995) developed an iterative model to calculate the elastic properties of shaly sandstones; however, their model cannot adequately account for the anisotropy in the reservoirs. Hornby et al. (1994) proposed an effective medium model to account for the anisotropy in shale reservoirs. Nonetheless, this model can only be used to determine the anisotropic characteristics of shale reservoirs at high-frequency conditions and is neither suitable for sandstone nor carbonate reservoirs, only for pure shale formations. Keys and Xu (2002) developed a model to calculate the elastic properties of shaly sandstones by using the pore characteristics of dry rocks but failed to account for anisotropy.

Based on the characteristics of the carbonate rock matrix and pore structure, and the effect of the latter on the elastic properties of carbonates, we developed an anisotropic effective medium model for carbonate reservoirs.

Method

Rock physical characteristics of carbonate rocks

There are several factors that affect the elastic properties of carbonates, such as the composition of the carbonate minerals, the porosity and shape of pores, the pore-fluid properties, saturation, temperature, pressure, seismic wave frequency, and so on. In general, the variation in carbonate mineralogy is small. The solid matrix of carbonates mainly consists of calcite, dolomite, aragonite, detrital minerals, anhydrite, and others. Therefore, the elastic properties of the carbonate matrix is nearly independent of mineral composition and the velocity of the carbonate frames can be approximately replaced by the mineral velocity when the porosity of the carbonates is very low.

Numerous measurements show that seismic wave propagation in carbonates is very complex. There is an obvious nonlinear relation between velocity and porosity even under laboratory conditions where the experimental frequency, temperature, pressure, and fluid properties can be precisely controlled, as shown in Figure 1. The scatter in the data is difficult to interpret by seismic wave theory or rock physics models. The porosity, pore size, pore shape, and pore connectivity in carbonates strongly affect the seismic wave velocity in carbonates.

Many researchers (Anselmetti et al., 1999; Asseffa et al., 2003; Eberli et al., 2003) have extensively studied the relation between carbonate pore type and seismic velocity by using laboratory experiments and theoretical models. The results show that the divergent relation between velocity and porosity can be reasonably modeled based on the pore structure. In general, the velocity of carbonates is high when

the pores are isolated and spherical, whereas the velocity is low in fractured carbonates. Anselmetti' s research (1999) showed that there are different velocity–porosity trends in carbonate samples with different pore shapes. The relation between velocity and porosity in carbonates can be grouped according to the pore structure of the samples. Figure 1 shows the relation between measured velocity and porosity of limestone samples from the TL area in the western basin of China. The measurements were conducted by using ultrasonic pulse transmission methods with work frequency at 0.8 kHzunder high temperature (100º~120º) and pressures (90 MPa~115MPa) to simulate the in situ formation condition. The data set consists of 370 samples of limestones and dolomitic limestones. The porosity of the samples is relatively low. The pores are intergranular, intragranular, ooid-like, and microcracks. The data scatter is high even at low porosity. Velocity differences as a function of porosity reach 1000 m/s when the porosity is greater than 2%, which likely reflects the stronger diversification in the pore structure of the carbonate samples in this group. Clearly, the pore structure of carbonates needs to be studied prior to building rock physics models.

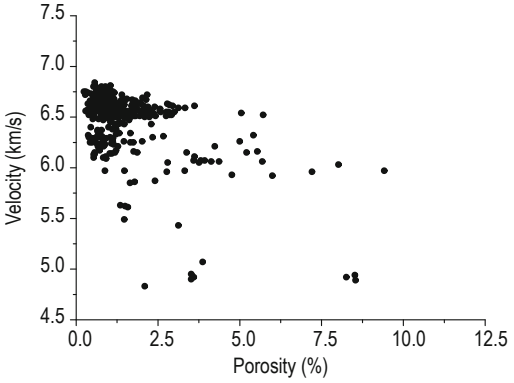

Fig.1 Measured velocity vs porosity in carbonate samples. Dots are the measured velocity and porosity of carbonate samples, the scatter in measured data indicates a variation in pore structures of carbonate samples.

Pore-structure model

There is no uniform classification for carbonate porosity owing to the complexity of the carbonate pore structure. Three categories are mainly used in industry. The Dunham (1962) classification is based on the rock grain texture. The Choquette and Pray (1970) classification is based on grain size, and the Lucia (1995) classification is based on the grain fabric and size. In the last two classification methods, the carbonate pores are divided into three categories according to the pore size: micropores with diameter less than 20 μm, middle pores with diameter around 20–100 μm, and large pores for pore diameter larger than 100 μm.

Intercrystaline pores, interparticle pores, intraparticle pores, moldic pores, vuggy, fenestral, growth-framework pores, and fractures are common in carbonate reservoirs. Among them, the shapes of intercrystaline and interparticle pores are commonly irregular. Intraparticle pores often appear in a single grain or open organic materials. Moldic porosity is due to the dissolution of organic materials in carbonates. Cracks are formed by stress variations, e.g., tectonic stress variations, cavity collapse, and abnormal changes in pore pressure, and so on. According to the carbonate pore classification and framework, the porosity of carbonates can be divided into primary and secondary porosity. Primary porosity is the portion of pore space that was present at the end of the deposition. Secondary porosity is created after the termination of deposition. Pore types, such as fractures and cavities, are secondary porosity. Rocks with intraparticle, or moldic, porosity and cavities are not easily deformed, whereas fractured rocks are more easily deformed, as shown in Figure 2.

A CT scanning image of a limestone sample, which was selected from a drilled well in the TL area, is shown in the upper left corner in Figure 2. The distribution of cracks is clearly seen in the CT scanning image (indicated by a red arrow). An image of the porosity of this sample is shown in the upper right corner of Figure 2. There are relatively well developed bioclasts in this sample. Cracks (indicated by arrows) and dissolved pores (indicated by the red circle) are also well developed at the microscopic scale. Most of the pores are isolated. Therefore, the effective porosity of the samples is very low. Electron microscope images of part of the sample are shown in the lower part of Figure 2. In the left, the image shows micropores within calcite and dolomite grains at 1000X magnification. In the right, the magnification is 2000X. The higher magnification image shows the shape of the calcite grains, contact pattern, and the distribution characteristics of the pores.

The classification of carbonate porosity, to some extent, reflects the deposition environment and the characteristics of diagenesis. Nonetheless, the classification schemes cannot fully describe the porosity heterogeneity and its effect on seismic wave velocity. Agersborg et al. (2005) showed that the relation between velocity and porosity in carbonate samples is related to the pore types, the size of pores and cracks, the connectivity of pores within the carbonate samples, and so on. Xu and Payne (2009) investigated the relation

between carbonate pore structures and P-wave velocity by improving the Xu–White model. Their results show that spherical pores, like moldic and dissolved pores, are associated with high velocity, whereas the velocity of fractured rock is relatively low. Kumar and Han (2005) divided the carbonate pore spaces into ellipsoids and fractures. By using isotropic differential effective medium models, they investigated the effect of pore shapes on velocity. The numerical results agreed well with published experimental data. Weger et al. (2004) suggested that carbonate elastic properties are closely related to pore size and complexity. Their study showed that carbonate pore shape, and pore size and sparsity strongly affect the elastic properties of carbonates.

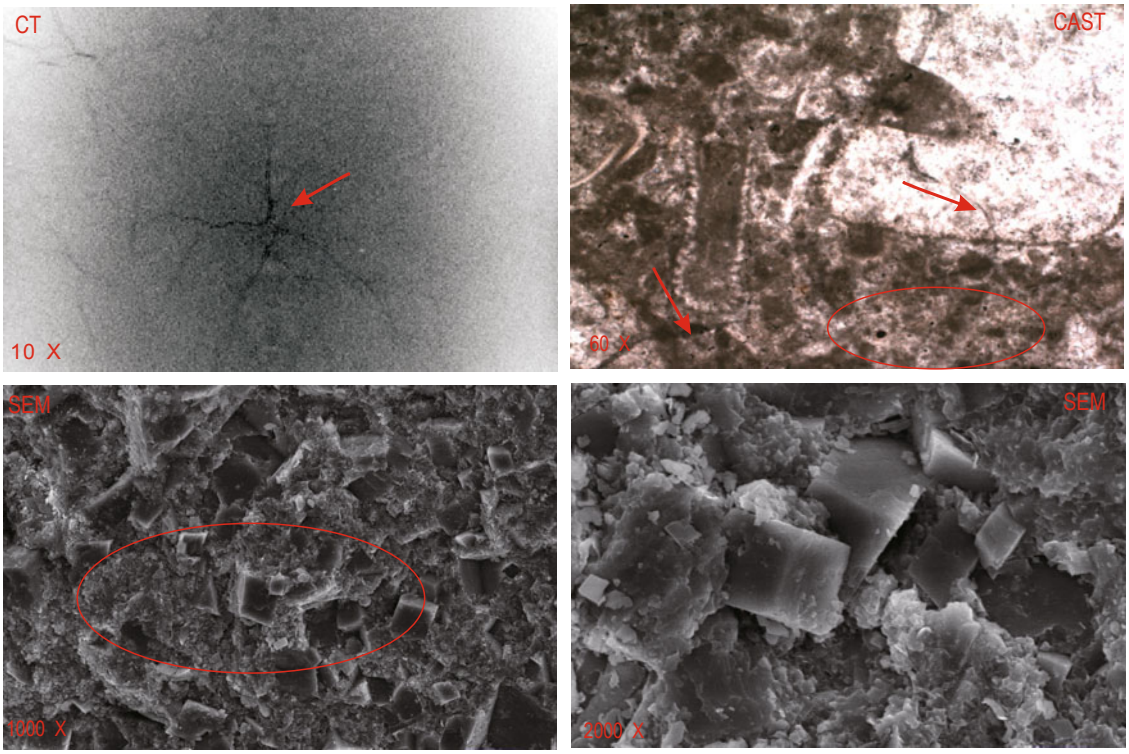

Fig.2 Pore structure of the carbonate samples in this study.

The red arrow in the upper left corner in Figure 2 indicates the fractures. The red arrows in the upper right corner indicate the fractures and there are some isolate pores in the red ellipse. In the lower part of figure 2 is the SEM result, in the left, there are micropores within calcite and dolomite grains (indicated by red ellipse), in the right, the image shows the shape of the calcite grains, contact pattern and the distribution characteristics of the pores.

Xu and Payne (2009) proposed a pore-structure model for carbonates, which divided the pore structure into four categories: pores filled with clays, intergranular pores, spherical pores, and fractures. Their pore model follows the Xu–White model; thus, there are differences compared with actual carbonates. First, carbonates typically consist of several minerals. The Hill model or SCA model can be used to characterize argillaceous limestones or argillaceous dolomites. Second, it is difficult to classify the intergranular, intragranular, and moldic porosity and the pore space of carbonates in practice. Furthermore, the interaction of grains with pore fluids and pore connectivity should be accounted for when the effect of pore fluids on the elastic properties is considered. Therefore, to build rock physics models for strongly heterogeneous carbonates, we need to synthesize data on pore structure (size, shape, and distributions), pore-filling materials, and pore connectivity.

Based on the measured data, the carbonate porosity can be divided into rigid pores that mostly consist of stiff ellipsoidal pores and soft pores that are mainly flexible fractures

$$\phi = \phi_s + \phi_f \text{ or } \phi = \phi_s + \phi_{f0} e^{-\beta\sigma},$$

where ϕ_s denotes the rigid pores, such as pores due to dissolution and some larger moldic, and interparticle pores. Ellipsoidal pores characterize this type of pore structure. The pore diameter is relatively large, second or third group in Lucia's classification. ϕ_f denotes the soft pores, which consists of microcracks around the particle edges and fractures induced by external forces. The

small pore aspect ratio is the characteristic of this pore structure. Fracture pores can be traced by experiments or logging data. ϕ_{f0} is the fracture porosity under atmospheric pressure, β is the gradient of the formation pressure, and σ is the stress. Other isolated micropores in rocks, including small intergranular and intragranular pores (the first category in Lucia's classification), are treated as inclusions in the rock matrix.

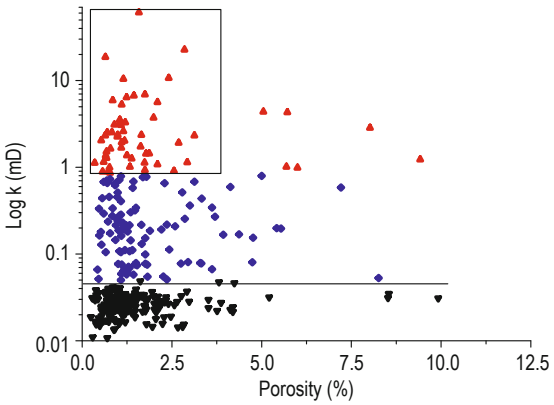

Fig.3 Permeability vs porosity of the carbonate samples used in this study.
Black dots indicate micropores, which are viewed as part of the solid matrix in the carbonates; red dots (related to fractures or cracks) indicate the soft pores; blue dots represent the rigid pores.

The pore-structure model is mainly based on following. Many unconnected micropores exist in the carbonate matrix. The micropores are mostly intracrystaline, intergranular, and intragranular pores (Figure 2). The diameter of the micropores is very small compared to the wavelength and the pores are randomly distributed. The effect of this pore structure on the rock elastic properties is negligible. In addition, the pore connectivity is poor (black points in Figure 3). Therefore, these micropores are viewed as part of the solid matrix of the carbonates. The measured data in Figure 3 are from drill core sections in the TL area. Fractures or cracks are relatively well developed owing to the brittleness of the carbonates. The fractured formation is easily identified in the porosity–permeability relation (red dots in Figure 3); low porosity corresponds to high permeability. The stiff pore, such as vugs and irregular pores, is an important and a major component of the effective porosity in carbonate reservoirs. Thus, the effective medium model of carbonates can be divided to two parts, that is , the rock matrix and pore space. The rock matrix includes various minerals and micropores, and the pore space consists of stiff pores and fracture-like soft pores. All pores within the pore spaces are connected.

The anisotropic effective medium model

Carbonate rocks, in contrast to sandstones, display complex pore structures with various pore shapes. The pore shape is the most significant rock property affecting the elastic property of the carbonate rocks. To investigate the effect of pore shapes on the elastic property of carbonate rocks, the effective medium theory was used. The most popular effective medium approaches are the self-consistent scheme (SC) and the differential effective medium scheme (DEM), which have the potential to capture the effect of pore shapes on elastic properties.

In particular, DEM is often used to model the elastic behavior of composite rocks. The DEM assume that the rock matrix has moduli K^0 and μ^0. The inclusion material has moduli K^i and μ^i. Then, the effective bulk and shear moduli of the composite are parameterized by $K^*(v)$ and $\mu^*(v)$, when the volume fraction of the inclusion phase is v. the isotropic form of DEM equation governing the changes in these constants are then to be

$$(1-v)\frac{dK^*(v)}{dv}=\left[K^i-K^*(v)\right]P^{*i} \tag{1}$$

and

$$(1-v)\frac{d\mu^*(v)}{dv}=\left[\mu^i-\mu^*(v)\right]Q^{*i}, \tag{2}$$

where the parameter v equals the inclusion volume fraction, the superscript i denotes the inclusion phase, the factors P^{*i} and Q^{*i} are the polarization factors for bulk and shear modulus. They depend on the bulk and shear moduli of both the rock matrix and inclusions, and the shapes of the inclusions.

In general, the isotropic form of DEM is regularly applied to analysis the effect of pore shapes on elastic properties of a composite. As mentioned above, there are unconnected and connected pores or fractures in carbonates, carbonate reservoir is often exhibited to be elastic anisotropy, it is not appropriate to use the isotropic form of DEM to model elastic behaviors of carbonate rocks with connected pores. To establish anisotropic carbonate rock physics model, we derived the anisotropic form of SC (equation (A-18) in Appendix A) and DEM model (equation (A-19) in Appendix A) , The detailed derivation is listed in Appendix A.

$$\mathbf{C}_{SCA}=\sum_{n=1}^{N}v_n\mathbf{C}^n\left(\mathrm{I}+\mathrm{E}(\mathbf{C}^n-\mathbf{C}_{SCA})\right)^{-1}\cdot\left(\sum_{m=1}^{N}v_m\left(\mathrm{I}+\mathbf{E}(\mathbf{C}^m-\mathbf{C}_{SCA})\right)^{-1}\right)^{-1} \tag{3}$$

and

$$(1-v)\frac{d}{dv}(\mathbf{C}_{DEM}(v)) = \left(\mathbf{C}^n - \mathbf{C}_{DEM}(v)\right)\left[\mathrm{I} + \mathrm{E}(\mathbf{C}^n - \mathbf{C}_{DEM}(v))\right]^{-1}, \quad (4)$$

where **C** is a fourth-order tensor, subscript SC denotes the self-consistent effective rigid tensor, subscript DEM represents the differential effective rigid tensor, the superscript *n* and *m* ($\mathbf{C}^n$ and $\mathbf{C}^m$) are the rigid tensors of the inclusions; I is the fourth-order identity tensor, E is the geometrical tensor, known as the Eshelby tensor (Eshelby, 1957), the scale N denotes the total number classes of inclusions, the scalar v is the inclusion volume fraction.

It is well known that isotropic form of DEM is suitable for modeling the elastic properties of a composite with idealized ellipsoidal inclusions, which are sufficiently sparse that they do not constitute any connected networks throughout the composite. It is imply that isotropic form of DEM can only be used to model the elastic properties of the carbonate with isolate pores or cracks. For real carbonate rocks, there are many cracks that connect different pores and fracture, which make it possible for hydrocarbon accumulation in carbonates. Therefore, it is appropriate to use the anisotropic form of DEM to model elastic behavior of carbonate reservoir with connected pore or fractures.

To compare the differences between the isotropic and anisotropic form of DEM, a numerical experiment was performed. A VTI (transverse isotropic with vertical axis of symmetry) model is assumed; the model consists of solid matrix and aligned pores filled with water. The solid matrix has a bulk modulus of 76 GPa, a shear modulus of 42 GPa, and density of 2.87 g/cm^3. The fluid component has a bulk modulus of 2.2 GPa, and density equal to 1.04 g/cm^3. The aspect ratio (AR) of inclusions is 0.05. The results are presented in Figure 4.

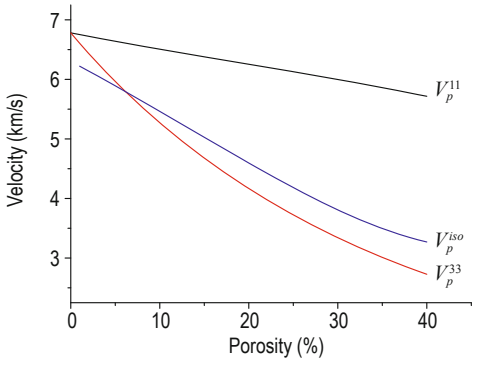

Fig.4 Predicted fluid-saturated P-wave velocity by anisotropic and isotropic DEM model.

In Figure 4, the V_p^{11} and V_p^{33} are calculated with the anisotropic effective elastic model (equation (4)), V_p^{11} represents the horizontal P-wave velocity and V_p^{33} denotes the vertical P-wave velocity; V_p^{iso} is firstly calculated with the isotropic form of DEM (equation (1) and (2)), then saturated with water by Gassmann's equation. We compare the effective elastic components calculated by the anisotropic form of DEM with the same modulus obtained by isotropic form of DEM. The comparisons of the velocity demonstrates that the velocity decrease with the increasing porosity. V_p^{iso} is always slower than V_p^{11}, but faster than V_p^{33} for porosity greater than 5%, and slower than V_p^{33} for porosity less than 5%. V_p^{11} is commonly greater than V_p^{33} for a VTI medium consisting of aligned horizontal fractures embedded in the solid matrix, implying that P waves propagate perpendicular to the axis of symmetry faster than parallel to the axis of symmetry. The result of comparisons implies that the elastic wave velocity in anisotropic rocks depends on the porosity of aligned inclusions.

Compared with isotropic DEM equation (1), anisotropic DEM equation (4) account not only for the change in velocity of different direction of seismic wave, but also for the relationship between velocity and oriented fractures. Isotropic media is a sampler specific case of anisotropy. In order to further evaluate the accuracy of equation (4) in the case of elastic anisotropic media. Measurements on fractured carbonate samples are used to compare with different DEM model.

Outcrop fractured carbonate rocks were used, three samples were taken (one oriented perpendicular, one parallel, and one oblique, to the dominant fracture direction) to include fracture anisotropy in each sample. P-wave and S-wave velocity, porosity and density measurement were made on the same samples. The average porosity and density of samples are 1.7% and 2.83 g/cc, respectively. The velocities of samples were measured both perpendicular ($V_P(0^\circ)$ and $V_{SH}(0^\circ)$), and parallel ($V_P(90^\circ)$ and $V_{SH}(90^\circ)$) to the direction of dominant fracture. A P-wave velocity was measured oblique ($V_P(45^\circ)$) to the dominant fracture. The elastic constant of anisotropic sample were calculated based on the measurements, as shows in Figure 5a.

$$c_{11} = \rho V_P^2(90^\circ), \quad c_{33} = \rho V_P^2(0^\circ),$$
$$c_{44} = \rho V_{SH}^2(0^\circ), \quad c_{66} = \rho V_{SH}^2(90^\circ), \quad (5)$$
$$c_{13} = \sqrt{4\rho^2 V_P^4(45^\circ) - 2\rho V_P^2(45^\circ)(c_{11}+c_{33}+2c_{44}) + (c_{11}+c_{44})(c_{33}+c_{44})} - c_{44}.$$

Figure 5a shows that outcrop samples drilled parallel to the dominant fracture had higher velocity than that of perpendicular to the dominant fracture, as expected. The P-wave anisotropy is significant, but the S-wave anisotropy is weak in the present samples. The seismic anisotropy show a decrease with increasing effective pressure because of the closure of compliant cracks in samples.

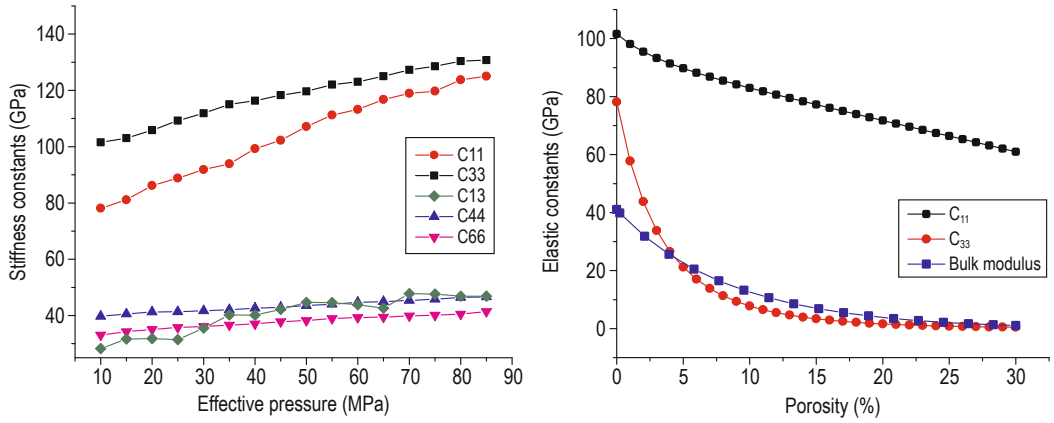

Fig.5 Analyzing the measurements of anisotropic sample with modelling results.
(a) stiffness constants vs effective porosity in carboanten samples; (b) comparison of the elastic moduli estimated by isotropic DEM with anisotropic DEM.

Based on the measured elastic parameters, the equation (1) and (4) were applied to investigate the difference in isotropic DEM and anisotropic DEM. For isotropic DEM model, the bulk modulus and shear modulus derived from the average of velocity both parallel and perpendicular to the dominant fracture are 42 GPa and 36 GPa. The stiff elastic tensor of matrix are selected from measured result at the effective pressure 20 MPa, with c_{11} = 101.56 GPa, c_{13} = 28.24 GPa, c_{33} = 78.16 GPa, c_{44} = 33.08 GPa and c_{66} = 39.73 GPa. The ellipsoidal inclusions with an aspect ratio to be 0.05 are used to mimic fractures within rocks, the porosity used in modeling is limited up to 30%. The result of numerical experiments shows in Figure 5b.

Figure 5b shows that there is a difference in isotropic DEM and anisotropic DEM. The bulk modulus calculated by isotropic DEM decrease with increasing fracture porosity. The elastic constant derived by anisotropic DEM in different wave propagation directions are sensitive to fracture porosity. The c_{11} has a slight decreasing with the change in fracture porosity, but c_{33} is sensitive to fracture porosities. The elastic modulus calculated by isotropic DEM is close to the elastic constant c_{33}.

The comparison demonstrates that measured velocities of fractured samples are sensitive to both the direction of oriented fractures and porosities. The elastic moduli calculated by isotropic DEM are less than c_{11} and greater than c_{33} (close to the elastic constant perpendicular to the dominant fracture). Application of isotropic form of DEM to analysis the elastic properties of anisotropic carbonate reservoirs in some cases overestimate actual effect of pore shapes on velocity and underestimate them in some others, resulting in incorrect interpretation of seismic response for carbonate reservoirs.

The workflow for carbonate rock physical modeling

To model the elastic parameters of cracked carbonate reservoirs by using anisotropic form of DEM, carbonate reservoirs is approximated as transversely isotropic, various minerals of carbonates are treated as isotropic. Then based on the volume fraction of minerals, the initial composite matrix is constructed by using anisotropic form of SC (equation (3)) iteratively, which can correctly handle the interaction between the different inclusions. The dry rock properties can be established by using anisotropic form of DEM model (equation (4)) according to the initial composite matrix. The anisotropic fluid substitution theory (Brown and Korringa, 1975) is used to fill pore fluid under anisotropic condition. Finally, the isolate micropores are added into the rock matrix by using Kuster-Toksoz model (Kuster and Tokson, 1974):

$$(\mathbf{K}^*_{KT}-\mathbf{K}^0)\frac{(\mathbf{K}^0-4\boldsymbol{\mu}^0/3)}{(\mathbf{K}^*_{KT}+4\boldsymbol{\mu}^0/3)}=\sum_{n=1}^{N}v_n(\mathbf{K}^n-\mathbf{K}^0)P^{mn} \quad (6)$$

and

$$(\boldsymbol{\mu}^*_{KT}-\boldsymbol{\mu}^0)\frac{(\boldsymbol{\mu}^0+\zeta)}{(\boldsymbol{\mu}^*_{KT}+\zeta)}=\sum_{n=1}^{N}v_n(\boldsymbol{\mu}^n-\boldsymbol{\mu}^0)Q^{mn}, \quad (7)$$

where

$$\zeta = \frac{\boldsymbol{\mu}^0(9\mathbf{K}^0 + 8\boldsymbol{\mu}^0)}{6(\mathbf{K}^0 + 2\boldsymbol{\mu}^0)},$$

where $\mathbf{K}^*_{KT}$ and $\boldsymbol{\mu}^*_{KT}$ are the bulk and shear modulus of the effective media, respectively, $\mathbf{K}^0$ and $\boldsymbol{\mu}^0$ are correspondingly the bulk and shear modulus of the composite matrix, and P^{mn} and Q^{mn} are geometrical coefficients that describe the effect of the nth inclusion on the background medium m, respectively.

We can also use Hudson's heterogeneous medium model to calculate the effective rigid tensor of composite media (Hudson, 1980)

$$\mathbf{c}^*_{hud} = \mathbf{c}^0_{ij} + \mathbf{c}^1_{ij}, \tag{8}$$

where $\mathbf{c}^*_{hud}$ denotes the effective rigid tensor of composite media, $\mathbf{c}^0_{ij}$ is the isotropic elastic tensor of media with homogeneous background and $\mathbf{c}^1_{ij}$ is the first-order correction if inclusions are present.

According to the procedure of constructing anisotropic rock physical model, a workflow based on the anisotropic effective medium theory to determine the effective elastic moduli or velocity of anisotropic carbonate rocks was proposed. The workflow comprises nine steps, as follow:

(1) Divide the carbonate rock into matrix and pore space. The pore space is then divided into stiff pores and fracture-like pores according to the porosity–permeability relation.

(2) The elastic tensor of the carbonate matrix is calculated according to the carbonate mineralogy. The rock matrix consists of various minerals that are distributed within the matrix.

(3) The stiff and flexible porosity are determined by measuring the porosity and permeability. In accordance with the formation pressure gradients, the fracture porosity is converted to in situ fracture formation. Thus, this process considers factors such as stress-induced anisotropy.

(4) The different pore shapes are determined according to the pore size and average aspect ratio of the fracture pores and stiff pores, respectively.

(5) Simulate the distribution of pores with variable shapes. Combine equations (3) and (4) to ensure pore connectivity and build a dry anisotropic composite elastic model.

(6) The elastic modulus of the pore fluid is determined by using the Wood equation.

(7) Using anisotropic fluid substitution theory (Brown and Korringa, 1975), the stiffness tensor of saturated anisotropic composite media is estimated according to the fluid modulus calculated by step 6 and the elastic model in step 5. The calculated stiffness tensor reflects the elastic characteristic of the composite medium at low frequency.

(8) The remaining micropores are then added into the rock matrix by using the Hudson or Kuster–Toksoz model, which treats micropores as isolated pores. These models have clear physical meaning and can be used to estimate the effect of the interaction between pore fluid and solid skeleton on the elastic properties of the composite medium.

(9) The symmetry axis of the anisotropic elastic model can be adjusted based on core imaging or well log imaging data.

Application of theoretical model

The theoretical prediction and measured data

The velocity of limestones is calculated by using the proposed method and thus the velocity–porosity relation is analyzed. Calcite and minor dolomite are the main minerals in the carbonate solid matrix. An anisotropic TI medium is established using equation (3). Fracture and spherical porosity are added by repeatedly using equation (4) with fixed fracture porosity of about 1% into the stiffness tensor determined with equation (3). Based on the in situ temperature and pressures, the brine bulk modulus is determined and then anisotropic fluid substitution is carried out using the Brown–Korrigna anisotropic fluid substitution model. A saturated anisotropic medium is established and, finally, the remaining micropores are added to the saturated anisotropic medium by using the Kuster–Tokzos equation assuming random distribution for the added pores. The results are shown in Figure 6.

The lower and upper Hashin–Shtrikman bounds are also shown in Figure 6. The pore shape is mainly controlled by the aspect ratio and pore concentration. By statistically analyzing the measured pore shapes in the carbonate samples, we found that the average aspect ratio of most micropores is around 0.15; thus, we use this value to characterize the velocity–porosity relations (indicated by red line in Figure 6). The velocity variation along the red line reflects the general relation between velocity and porosity of the carbonate samples. At the same porosity range, the velocity deviates from the trend line and increases along the red up-arrow in Figure

6 when spherical pores (cavity or vugs) are relatively well developed. In contrast, the down-arrow in Figure 6 shows the decreasing velocity when pore shapes become flat.

The relation between velocity and porosity of carbonates suggests that the larger the pore aspect ratio is, the greater the rock resistance to deformation is, and thus the velocity increases. In contrast, carbonate velocity decreases because of fracture pores. We compared the theoretical prediction with the measured data. The results are shown in Figure 7.

Figure 7 shows that the majority of the measured data are distributed around the AR = 0.15 line, whereas the rest of the data, as expected, fall on the velocity–porosity trend lines for fractured samples. By comparing the theoretical prediction with the measured data in Figure 7, we can see that the proposed anisotropic theoretical model provides the basis for qualitatively analyzing the pore structure of carbonate reservoirs and fracture zones.

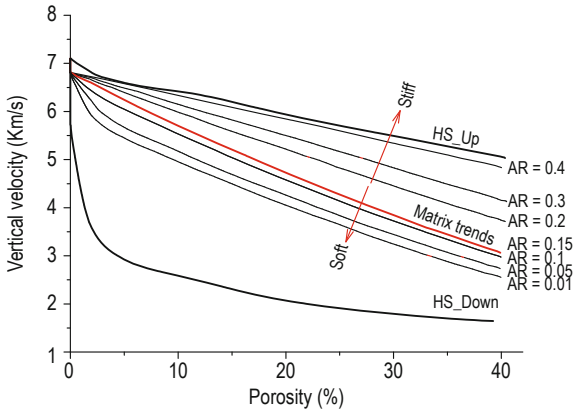

Fig.6 Model velocity-porosity relations

The red line characterizes the velocity-porosity trends of carbonate matrixes. The velocity increases along the red up arrow when more stiff pores are relatively well developed. In contrast, the red down arrow shows the decreasing velocity when soft pores are developed.

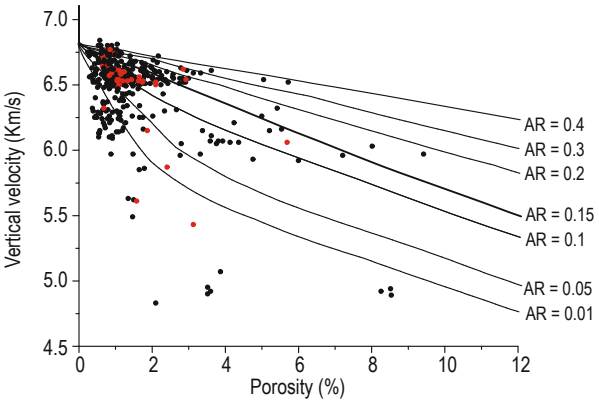

Fig.7 Measured data vs theoretical predictions.

The solid lines are the theoretically predicted trends using the proposed elastic model. The points are the measured data in the limestone samples. The red points are identical to the red dots in Figure 3 and are the measured data for fractured samples observed in thin sections.

The theoretical prediction and well data

Figure 8 shows the velocity–porosity relation of well data in the TL area. The velocity trends in Figure 6 are also shown. The data in Figure 8 represent the velocity and porosity of the limestone sections under investigation.

As shown in Figure 8, the logging velocity–porosity data are clustered in the low-porosity–low-velocity region. The natural Gamma Ray log (GR) readings are generally less than 30 API, whereas the fractured limestone GR readings are less than 15 API. Logging data with GR less than 13 API mostly fall below the theoretical trend line with AR equal to 0.05. Logging data with higher GR values are located in the region of relatively high aspect ratio. The results of imaging logging in lower aspect ratio region suggest that fractures are relatively well developed in this interval. However, the results of imaging logging in higher aspect ratio region suggest that there are some caves in the formation. The comparison between logging data and theoretical modeling results shows that the anisotropic

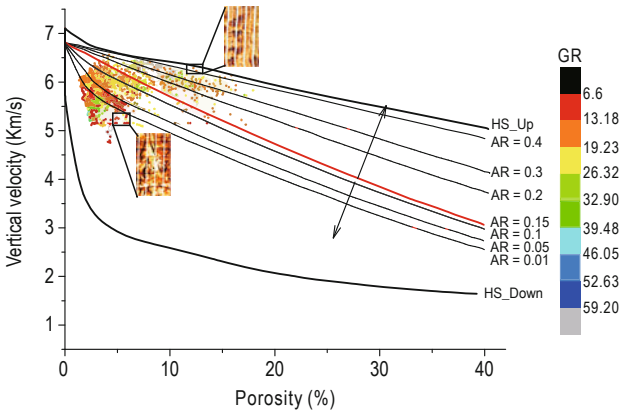

Fig.8 Comparison of theoretical predictions and well log data.

The solid lines are the theoretically predicted trends same as in Figure 6. The color dots are logging velocity and porosity coded by Gamma Ray readings. The red line represents the properties of carbonate matrixes. The logging data in higher aspect ratio region suggest that there are some stiff pores demonstrated by the imaging logging result as shows in the upper part of Figure 8. However, the logging data in lower aspect ratio region suggest that there are some soft pores or fractures demonstrated by the imaging logging result as shows in the lower part of Figure 8.

theoretical model can be used to analyze the relation between velocity and porosity of carbonate reservoirs and evaluate carbonate formations.

Conclusions

We developed an anisotropic effective theoretical model for carbonate reservoirs based on effective medium theory. We also proposed a workflow for estimating the elastic properties of anisotropic composites. Compared with conventional isotropic models, the advantage of the proposed anisotropic model is that it can estimate the effective elastic tensor of anisotropic media. The anisotropic self-consistent approximate model and differential effective medium model developed in this study can calculate and analyze the interaction between inclusions within composite media, and provide a reasonable basis for anisotropic fluid substitution. Therefore, the proposed anisotropic model is more suitable for calculating and analyzing the elastic properties of anisotropic carbonate reservoirs.

By analyzing the pore-structure characteristics of thin sections of carbonate samples in the TL area, a pore-structure model for carbonate rocks was proposed, which accounts for the pore shape, size, and other parameters. Carbonates were divided into the pore and solid domain. The pore domain consists of fracture-like soft pores and stiff pores; the solid domain comprises minerals and isolated micropores. This pore-structure model can be used to distinguish fractures from the rest of the pores using known velocity–porosity data in carbonate reservoirs when no prior information of the pore structure is available. Thus, it offers the possibility to predict fractured sections by using seismic data.

We described the steps for estimating the anisotropic elastic tensor for carbonate reservoirs in terms of the pore-structure model and the anisotropic effective theoretical model. We used this approach to analyze the relation between velocity and porosity in carbonate rocks. The comparison of model predictions and measured data in carbonate samples showed that the proposed method can determine the velocity–porosity pattern in limestone reservoirs with variable pore shapes. However, the proposed method needs to be carefully calibrated before assessing reservoir by seismic velocity and porosity.

The proposed method provides a novel method for analyzing carbonate reservoirs. The anisotropic effective theoretical model forms the basis for developing new technologies for seismic data prediction and interpretation in fractured sections.

Acknowledgment

The authors would like to thank Lv Hua-Xing and Liu Yang for their help in preparing this paper. We also thank the anonymous reviewers for reviewing the manuscript and helpful suggestions.

References

Agersborg, R. T., Hohansen, A., and Jakobsen, M., 2005, The T-matrix approach for carbonate rocks: 75th Ann. Internat. Mtg., Soc. Explor. Geophys., Expanded Abstracts, 1597–1600.

Anselmetti, F., and Ebrili, G. P., 1999, The velocity-deviation log: A tool to predict pore type and permeability trends in carbonate drill holes from sonic and porosity or density log: AAPG Bulletin, **83**(3), 450–466.

Asseffa, S., McCann, C., and Sothcott, J., 2003, Velocity of compressional and shear waves in limestones: Geophysical Prospecting, **51**(1), 1–13.

Brown, R., and Korringa, I., 1975, On the dependence of elastic properties of a porous rock on the compressibility of the pore fluid: Geophysics, **40**(4), 608–616.

Budiansky, B., 1965, On the elastic moduli of some heterogeneous materials: J. Mech. Phys. Solid, **13**(4), 223–227.

Carcione, J. M., and Avseth, P., 2015, Rock-physics templates for clay-rich source rocks: Geophysics, **80**(5), D480–500.

Castagna, J., Batzle, M., and Eastwood, R., 1985, Relationships between compressional-wave and shear-wave velocity in clastic silicate rocks: Geophysics, **50**(4), 571–581.

Choquette, P. W., and Pray, L. C., 1970, Geologic nomenclature and classification of porosity in sedimentary carbonates: AAPG Bulletin, **54**(2), 207–244.

Christensen, R. M., 2005, Mechanics of composite materials: Wiley, New York, 31–71.

Dunham, R. J., 1962, Classification of carbonate rocks according to depositional texture: AAPG Bulletin, **46**(1), 108–121.

Eberli, G. P., Baechle, G., Anselmetti, F., Incze, M., Dong, W., Tura, A., and Saparkman, G., 2003, Factors controlling elastic properties in carbonate sediments and

rocks: The Leading Edge, **22**(7), 654–660.
Eshelby, J. D., 1957, The determination of the elastic field of an ellipsoidal inclusion, and related problem: Proc. Roy. Soc, **A241**(1226), 376–396.
Hornby, B. E., Schwartz, M., and Hundson, A., 1994, Anisotropic effective-medium modeling of the elastic properties of shales: Geophysics, **59**(10), 1570–1583.
Huang, H., Stewart, R. R., Sil, S., and Dyaur, N., 2015, Fluid substitution effect on seismic anisotropy: J. Geophys. Res, **120**(2), 850–863.
Hudson, J. A., 1980, Overall properties of a cracked soild: Mathematical Proceedings of the Cambridge Philosophical Society, **88**(2), 371–384.
Keys R. G., and Xu, S., 2002, An approximation for the Xu-White velocity model. Geophysics, **67**(5), 1406–1414.
Krief, M., Garat, J., Stellingwerff, J., and Ventre, J., 1990, A petrophysical interpretation using the velocities of P and S waves (full waveform sonic): The Log Analyst, **31**(6), 355–369.
Kumar M., and Han, De-hua, 2005, Pore shape effect on elastic properties of carbonate rocks: 75th Ann. Internat. Mtg., Soc. Explor. Geophys., Expanded Abstracts, RP1.3, 1477–1480.
Kuster, G. T., and Toksoz, M. N., 1974, Velocity and attenuation of seismic waves in two-phase media:Part I: Theoretical formulations: Geophysics, **39**(5), 587–606.
Landro, M., 2015, Aspect ratio histograms of 3D ellipsoids and 2D ellipses—Analytical relations and numerical examples: Geophysics, **80**(2), D429–D440.
Li, J. Y., and Chen, X. H., 2013, A rock-physical modeling method for carbonate reservoirs at seismic scale: Appl. Geophys., **10**(1), 1–13.
Lucia, F. J., 1995, Rock-fabric/petrophysical classification of carbonate pore space for reservoir characterization: AAPG Bulletin, **79**(9), 1275–1300.
Mavko, G., Mukerkji T., and Dvorkin, J., 2001, The rock physics handbook: Tools for seismic analysis inporous media: Cambridge University Press, New York, 169–224.
Regnet, J. B., Robion, P., David, C., Fortin, J., Brigaud, B., and Yven B., 2015, Acoustic and reservoir properties of microporous carbonate rocks: Implication of micrite particle size and morphology, J. Geophys. Res, **120**, 790–811.
Walpole, L. J., 1969, On overall elastic moduli of composite materials: J. Mech. Phys. Sol., **17**(4), 235–251
Weger, R. J., Baechle, G. T., Masaferro, J. L., and Everli. G. P., 2004, Effect of porestructure on sonic velocity in carbonate: 74th Ann. Internat. Mtg., Soc. Explor. Geophys., Expanded Abstracts, 1774–1777.
Willis, J. R., 1977, Bounds and self-consistent estimates for the overall properties of anisotropic composites: J. Mech. Phys. Solids, **25**(3), 185–202.
Xu S., and Payne, M. A., 2009, Modeling elastic Properties in carbonate rocks: The Leading Edge, **28**(1), 66–74.
Xu, S., and White, R. E., 1995, A new velocity model for shear-wave velocity prediction: Geophysical Prospecting, **43**(1), 91–118.
Yu, H., Ba, J., Carcione, J., Li, J. S., Tang, G., Zhang, X. Y., He, Z. H., and Ouyang, H., 2014, Rock physics modeling of heterogeneous carbonate reservoirs: porosity estimation and hydrocarbon detection: Appl. Geophys., **11**(1), 9–22.

Appendix A

We assume that the matrix of a composite materials occupying a volume V, is subject to boundary displacement that is compatible with the volumetric average strain $\langle \mathbf{e} \rangle$ throughout V. Furthermore, there are different homogeneous inclusions with different properties in the composite media. The volumetric average stress $\langle \boldsymbol{\sigma} \rangle$ within V is given by (Christensen, 2005)

$$\langle \boldsymbol{\sigma} \rangle = \mathbf{C}^* \langle \mathbf{e} \rangle, \tag{A-1}$$

where $\mathbf{C}^*$ is the overall elastic tensor of the materials and $\langle \cdot \rangle$ indicates volumetric averages of the enclosed properties.

We assume that the compliance tensor does not change when the composite medium experiences external forces, and the average strain and stress of the composite medium is (Christensen, 2005)

$$\langle \mathrm{e} \rangle = \frac{1}{V} \sum_{n=0}^{N} \int_{V_n} \mathrm{e}_{ij}(x) dV \tag{A-2}$$

and

$$\langle \boldsymbol{\sigma} \rangle = \frac{1}{V} \sum_{n=0}^{N} \int_{V_n} \boldsymbol{\sigma}_{ij}(x) dV, \tag{A-3}$$

where $\mathbf{e}_{ij}(x)$ and $\boldsymbol{\sigma}_{ij}(x)$ are the local strain and stress at position x, respectively, N denotes the number of

inclusions, V is the volume of the composite medium, and Vn is the volume of inclusions.

We define the average stress and strain in the nth inclusion as

$$V_n\boldsymbol{\sigma}^n = \int_{V_n} \boldsymbol{\sigma} dV \tag{A-4}$$

and

$$V_n\mathbf{e}^n = \int_{V_n} \mathbf{e} dV, \tag{A-5}$$

where $\boldsymbol{\sigma}^n$ and $\mathbf{e}^n$ are the average strain and stress in the nth inclusion, respectively. The constitutive equation for the inclusions can be written as (Christensen, 2005)

$$\boldsymbol{\sigma}^n = \mathbf{C}^n\mathbf{e}^n, \tag{A-6}$$

where $\mathbf{C}^n$ is a fourth-order elastic stiffness tensor and

$$\langle \mathrm{e} \rangle = \sum_{n=0}^{N} v_n\, \mathrm{e}^n \tag{A-7}$$

and

$$\langle \boldsymbol{\sigma} \rangle = \sum_{n=0}^{N} v_n \boldsymbol{\sigma}^n = \sum_{n=0}^{N} v_n \mathbf{C}^n\mathbf{e}^n, \tag{A-8}$$

where v_n is the volume fraction of the nth inclusion.

We isolate the elastic moduli of the matrix from the overall elastic tensor and express

$$\langle \boldsymbol{\sigma} \rangle = \mathbf{C}^0 \langle \mathbf{e} \rangle + \sum_{n=1}^{N} v_n \left(\mathbf{C}^n - \mathbf{C}^0 \right) \mathbf{e}^n, \tag{A-9}$$

where $\mathbf{c}^0$ is the elastic stiffness tensor of the matrix of the composite medium.

Following the analysis of Willis (1977), the values of $\mathbf{e}^n$ are estimated by embedding an isolated inclusion with moduli $\mathbf{C}^n$ subjected to average strain $\langle \mathbf{e} \rangle$ far from the inclusion. We define the tensor $\mathbf{T}^n$ that relates $\mathbf{e}^n$ to the average strain $\langle \mathbf{e} \rangle$ as

$$\mathrm{e}^n = \mathbf{T}^n \langle \mathbf{e} \rangle, \tag{A-10}$$

where $\mathbf{T}^n$ depends on the stiffness tensors $\mathbf{C}^n$ and $\mathbf{C}$. We substitute equation (10) to equation (9) and we obtain

$$\langle \boldsymbol{\sigma} \rangle = \left\{ \mathbf{C}^0 + \sum_{n=1}^{N} v_n \left(\mathbf{C}^n - \mathbf{C}^0 \right) \mathbf{T}^n \right\} \langle \mathbf{e} \rangle. \tag{A-11}$$

By comparing equations (1) and (11), the effective stiffness tensor for heterogeneous media is obtained

$$\mathbf{C}^* = \mathbf{C}^0 + \sum_{n=1}^{N} v_n \left(\mathbf{C}^n - \mathbf{C}^0 \right) \mathbf{T}^n. \tag{A-12}$$

For ellipsoidal inclusions, $\mathbf{T}^n$ is explicitly given as (Willis, 1977)

$$\mathbf{T}^n = \left[\mathbf{I} + \mathbf{E}(\mathbf{C}^n - \mathbf{C}^0) \right]^{-1}, \tag{A-13}$$

where $\mathbf{I}$ is the fourth-order identity tensor and $\mathbf{E}$ is the pore-shape tensor, known as the Eshelby tensor (Eshelby, 1957).

Be substituting equation (13) to equation (12), we obtain

$$\mathbf{C}^* = \mathbf{C}^0 + \sum_{n=1}^{N} v_n \left(\mathbf{C}^n - \mathbf{C}^0 \right) \left[\mathbf{I} + \mathbf{E}(\mathbf{C}^n - \mathbf{C}^0) \right]^{-1}. \tag{A-14}$$

To determine the elastic tensor of composite media, the stiffness tensor of each inclusion must be determined first.

If the inclusions are homogeneous and randomly distributed, the effective elastic properties of composite media can be calculated by using the isotropic SCA or DEM model (Mavko et al., 2001). However, these isotropic effective models actually represent the elastic behavior of composite media with isolated inclusions. There are different pore pressures within each inclusion. Therefore, isotropic effective models cannot calculate the elastic properties of actual carbonate reservoirs with connected fractures and cavities at seismic frequencies. To describe heterogeneous composite media with connected pores, we first need to account for the equilibration of pore pressure and then to determine the elastic tensors.

According to self-consistent models (Budiansky, 1965), when we consider fully connected composite media, we can use the self-consistent effective rigid tensor $\mathbf{C}_{SCA}$ to replace the matrix tensor $\mathbf{C}^0$ of the composite media.

Following Walpole (1969), a homogeneous material with moduli $\mathbf{C}^0$ is introduced and the polarization $\boldsymbol{\tau}^n$ is defined as

$$\boldsymbol{\tau}^n = \left[(\mathbf{C}^n - \mathbf{C}^0)^{-1} + \mathbf{E} \right]^{-1} \langle \mathbf{e} \rangle, \tag{A-15}$$

this then gives

$$\langle \boldsymbol{\sigma} \rangle = \mathbf{C}^* \langle \mathbf{e} \rangle + \boldsymbol{\tau} = \mathbf{C}^* \langle \mathbf{e} \rangle + \sum_{n=1}^{N} v_n \left[(\mathbf{C}^n - \mathbf{C}^0)^{-1} + \mathbf{E} \right]^{-1} \langle \mathbf{e} \rangle. \tag{A-16}$$

It follows that

$$\sum_{n=1}^{N} v_n \left[(\mathbf{C}^n - \mathbf{C}_{SCA})^{-1} + \mathbf{E} \right]^{-1} = 0, \qquad \text{(A-17)}$$

or, by rearranging,

$$C_{SCA} = \sum_{n=1}^{N} v_n C^n \left(\mathrm{I} + \mathrm{E}(C^n - C_{SCA}) \right)^{-1} \cdot \left(\sum_{m=1}^{N} v_m \left(\mathrm{I} + \mathrm{E}(C^m - C_{SCA}) \right)^{-1} \right)^{-1}. \qquad \text{(A-18)}$$

When using the DEM model to calculate the effective tensor of anisotropic media, we set the incremental volume Δv of the inclusions with volume v; thus, the elastic tensor of the composite media can be expressed according to equation (14) as

$$(1-v)\frac{d}{dv}(\mathbf{C}_{DEM}(v)) = \left(\mathbf{C}^n - \mathbf{C}_{DEM}(v)\right)\left[\mathrm{I} + \mathrm{E}(\mathbf{C}^n - \mathbf{C}_{DEM}(v)) \right]^{-1}, \qquad \text{(A-19)}$$

where the fourth-order tensor $\mathbf{C}_{DEM}$ is the differential effective rigid tensor.

Li Sheng-Jie received his PhD from the Department of Geophysics, University of Science and Technology of China in 2003. He is an associate professor at the College of Geophysics and information engineering, the China University of Petroleum. His interests are seismic rock physics, reservoir characterization, and seismic interpretation.

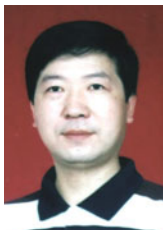

(Edited by Hu Tian-Yue)